RET and Anisotropy Measurements Establish the Proximity of the Conserved Trp17 to Ile98 and Phe99 of Tear Lipocalin†

Oktay K. Gasymov, Adil R. Abduragimov, Taleh N. Yusifov, and Ben J. Glasgow*

Departments of Pathology and Ophthalmology, University of California at Los Angeles School of Medicine, Los Angeles, California 90095

Received November 29, 2001

ABSTRACT: Previous studies suggest that the conserved Trp17 on strand A of TL has a role in lipocalin stability and interacts, directly or indirectly, with Ile98 and Phe99 on strand G to influence ligand binding. Here, we determined the proximity of Trp17 to Ile98 and Phe99. Time-resolved fluorescence experiments showed resonance energy transfer between tryptophans at positions 17 and 98. In addition, an exciton effect was discovered in CD experiments resulting from interactions of the excited states of these tryptophans. Fluorescence anisotropy values of mutants containing two tryptophans (positions 99/17 and 98/17) were lower than expected in the absence of RET, confirming that these residues are proximate in tear lipocalin. The data support a model of tear lipocalin in which Trp17 and Phe99 are close together deep in the cavity and participate in an internal hydrophobic cluster. Ile98 is proximate to Trp17 but faces toward the outside of the cavity and in the model is part of an external hydrophobic patch. Comparison with β-lactoglobulin suggests that these motifs may have an important influence on protein stability and ligand binding in other members of the lipocalin family.

TL[1] is the principal lipid binding protein in tears and carries fatty acids, glycolipids, phospholipids, and cholesterol (*1*). Putative functions for TL include scavenging lipid from the corneal surface to prevent the formation of lipid-induced dry spots (*2*), solubilization of lipid in tears (*2*), antimicrobial activity (*3*), cysteine proteinase inhibition (*4*), transport of sapid molecules in saliva (*5*), transport of retinol in tears (*6*), scavenging of potentially harmful lipid oxidation products (*7*), and endonuclease activity (*8*). Common to each of these diverse functions is the binding of a ligand or substrate.

Lipocalin family members exhibit a wide range of functions that have been deduced from the type of ligand. For most lipocalins, ligand binding occurs within the lipocalin fold (*9*). The lipocalin fold is a large cup-shaped cavity that exists within an eight-stranded antiparallel β-sheet. The sheet is closed back on itself to form a continuously hydrogen-bonded β-barrel. The binding sites for a few ligands have been established in crystallographic studies of several lipocalins. β-Lactoglobulin has been the most extensively studied. Ragona et al. identified 11 amino acid residues of β-lactoglobulin that form a hydrophobic cluster and perhaps an internal binding site (*10*). This cluster of hydrophobic residues may be important in providing a stabilizing core that is resistant to denaturation (*11*). In addition, an external hydrophobic patch may act as an external binding site (*10*).

Although the crystal structure of TL has not yet been revealed, the secondary structure of the entire protein has been resolved by site-directed tryptophan fluorescence (SDTF) and in part validated by site-directed spin labeling (*12*−*14*). On the basis of SDTF data, a three-dimensional (3D) homology model for TL has been constructed (*12*). Comparison of the analogous regions of β-lactoglobulin and TL permits the hypothesis that key residues in TL may form hydrophobic groups that influence protein conformation and ligand binding. In the model of TL, residues Trp17, Phe99, and Ile98 occupy positions analogous to Trp19, Leu103, and Try102 of β-lactoglobulin, respectively. Trp19 and Leu103 are positioned in an internal hydrophobic cluster, and Tyr102 is located in an external hydrophobic patch of β-lactoglobulin (*10*). Evidence is mounting that these positions are critical for the structure−function relationships of TL. Trp17 is the sole tryptophan in TL. Trp17 is relatively inaccessible to solvents in both the holo- and apo-TL forms (*15*). Lipid binding produces structural and conformational alterations that involve Trp17. Replacement of Trp17 with a nonaromatic residue is accompanied by a reduction in the extent of β-structure formation and aromatic side chain asymmetry, decreased binding affinity for fatty acids, and destabilization of tear lipocalin upon denaturation (*16*). Trp17 appears to be important in stabilization of TL and ligand binding. It is plausible that this residue exists at the core of an internal hydrophobic cluster.

Phe99 in TL is analogous to Leu103 in β-lactoglobulin and is deeply buried in tear lipocalin. Phe99 has a motionally restricted side chain and is relatively inaccessible to acrylamide, NiEDDA, and oxygen (*13*, *14*). Tear lipocalin bearing

† Supported by U.S. Public Health Service Grant EY 11224 and an unrestricted grant from Research to Prevent Blindness to B.J.G.

* To whom correspondence should be addressed: 100 Stein Plaza, Rm B-279, Los Angeles, CA 90095. Fax: (310) 794-2144. Phone: (310) 825-6998. E-mail: bglasgow@mednet.ucla.edu.

[1] Abbreviations: C12SL, spin-labeled analogue of lauric acid; CD, circular dichroism; DAUDA, 11-({[5-(dimethylamino)-1-naphthalenyl]-sulfonyl}amino)undecanoic acid; λ_{max}, fluorescent emission maximum; RBP, retinol binding protein; SDTF, site-directed tryptophan fluorescence; TL, tear lipocalin; UV, ultraviolet; NATA, *N*-acetyl-L-tryptophanamide; SCM, spectral center of mass; RET, resonance energy transfer; WT, expressed wild-type tear lipocalin.

10.1021/bi0121003 CCC: $22.00
Published on Web 06/19/2002

the mutation F99C exhibits decreased overall aromatic side chain asymmetry as well as reduced asymmetry specifically contributed by Trp17 (*14*). SDTF data show that Trp at position 99 has the second most blue shifted emission maximum (325 nm) of all β-strand residues in the entire lipocalin molecule (*12*). Therefore, Phe99 is a likely participant in an internal hydrophobic cluster and may be in the proximity of Trp17.

Ile98 on the G strand of TL is analogous to Tyr102 in β-lactoglobulin. In β-lactoglobulin, a hydrophobic surface patch (Leu22, Ala23, Tyr42, Tyr102, and Leu104), which is located in a groove between the strands and main α-helix, was suggested as a possible external binding site (*10*). The TL model suggests that the side chain of Ile98 faces out from the cavity. A close relationship is implied between Ile98 and Trp17 because the mutant I98C shows a marked decrease in optical activity in the region of the chromophore absorption band of Trp17 (*14*). Using a nitroxide spin-label at position 98 and a fast relaxing reagent, both mobile and motionally restrained populations have been identified (*14*). These data suggest that Ile98 exhibits tertiary side chain interactions with another strand and may account for susceptibility to structural alterations. Mutation at positions 17 or 98 with a nonaromatic residue greatly enhances retinoid binding presumably by relaxation of the putative hydrophobic cluster that in turn permits better accommodation of the β-ionone ring (unpublished data).

Together, these data point to the existence of functional and structural interrelationships among residues Trp17, Ile98, and Phe99. The 3D model of tear lipocalin suggests proximity between the residues [Ile98 (CB)−Trp17 (CZ3) = 5.53 Å and Phe99 (CB)−Trp17 (CH2) = 3.84 Å] (*12*). These distances are particularly suitable for detecting resonance energy transfer between the two tryptophans as well detection of an exciton effect in CD spectra. The purpose of this study is to determine experimentally if the proximity of Trp17 to Phe99 and Ile98 is consistent with a model in which Phe99 and Trp17 are positioned in a hydrophobic cluster and Ile98 is positioned in an external hydrophobic patch.

EXPERIMENTAL PROCEDURES

Site-Directed Mutagenesis and Plasmid Construction. The TL cDNA in PCR II (Invitrogen, San Diego, CA), previously synthesized (*17*), was used as a template to clone the TL gene spanning bases 115−592 of the previously published sequence (*6*) into pET 20b (Novagene). Flanking restriction sites for *Nde*I and *Bam*HI were added to produce the native protein sequence as found in tears (*18*). To avoid the use of subtraction spectra in analysis and to simplify the interpretation of quenching experiments in molecules with substituted tryptophans, it was first necessary to substitute the native tryptophan with an amino acid that did not induce significant structural perturbations and has similar binding characteristics (*13*, *16*). We prepared a TL mutant, W17Y, with oligonucleotides (Universal DNA Inc.) using the previously published method of introduction of a point mutation by sequential PCR steps (*19*). Using this mutant as a template, mutant cDNAs were constructed in which the corresponding amino acids were additionally substituted sequentially with tryptophan. Amino acid 1 corresponds to His, bases 115−118 according to Redl (*6*).

Expression and Purification of Mutant Proteins. The mutant plasmids were transformed in *Escherichia coli* BL21-(DE3); cells were cultured, and protein was expressed according to the manufacturer's protocol (Novagene). Following cell lysis (*20*), the supernatant was treated with methanol (final concentration of 40%) at 4 °C for 2.5 h. Alternatively, mutant proteins expressed in inclusion bodies were dissociated in 8 M urea at room temperature for 2 h. In either case, the resulting suspension was centrifuged at 3000*g* for 30 min. The supernatant was dialyzed against 50 mM Tris-HCl (pH 8.4). The dialysate was treated with ammonium sulfate (45−75% saturation). The resulting precipitate was dissolved in 50 mM Tris-HCl (pH 8.4) and applied to a Sephadex G-100 column (2.5 cm × 100 cm) equilibrated with 50 mM Tris-HCl and 100 mM NaCl (pH 8.4). The fraction containing the mutant protein was dialyzed against 50 mM Tris-HCl (pH 8.4) and applied to a DEAE-Sephadex A-25 column. Bound protein was eluted with a 0 to 0.8 M NaCl gradient. Eluted fractions containing mutant proteins were centrifugally concentrated (Amicon, Centricon-10). The purity of mutant proteins was verified by SDS tricine gel electrophoresis (*1*). The protein concentration was determined by the biuret method (*21*). For ligand binding experiments, delipidation of WT and mutant proteins were performed as previously described (*1*).

Absorption Spectroscopy. UV absorption spectra were recorded at room temperature using a Shimadzu UV-2400PC spectrophotometer. The spectra were corrected for turbidity by plotting the dependence of the log of the absorbance of the solution versus the log of the wavelength and extrapolating the linear dependence between these quantities in the range of 320−360 nm to an absorption range of 240−320 nm.

EPR Measurements. Electron paramagnetic resonance spectra were recorded at X-band with a Varian E-109 spectrometer fitted with a two-loop one-gap resonator (*22*). Samples (5 μL) were loaded in 0.84 mm outside diameter capillaries (Vitrocom Inc., Mountain Lakes, NJ) that were sealed at one end. All spectra were acquired at X-band using an incident microwave power of 2 mW and a scan width of 100 G. Acquisition and manipulation of EPR spectra were carried out using computer programs written in LabVIEW (National Instruments, Austin, TX) by C. Altenbach. The modulation amplitude was 1 G and the time constant 0.3 s. Signal averaging was performed with 30 scans. For ligand binding, a stock solution of C12SL was prepared in ethanol (*1*). A constant concentration of WT was titrated with progressively increasing concentrations of C12SL or mutant proteins, and the EPR spectra were recorded. The final concentration of ethanol did not exceed 2%. The EPR spectra revealed the presence of both the free spin-label and that bound to protein. The ratio of bound to free spins in equilibrium was estimated by spectral titration (*1*). The free spectrum of the spin-label was subtracted from a composite spectrum of bound and free to give the pure bound spectrum. The ratio of double integrals of the pure bound to pure free gave the bound to free molar ratio. The concentrations of the spin-label in solution, calculated by double integration of the EPR spectra, were compared with that of a standard solution of Tempol (*1*). The Scatchard plots were fitted by standard nonlinear regression techniques (using ORIGIN,

Microcal, Northampton, MA) to a linear curve to give estimates of the dissociation constant (K_d).

CD Spectral Measurements. Spectra were recorded (Jasco 600 spectropolarimeter, 0.2 and 10 mm path lengths for far- and near-UV spectra, respectively) using protein concentrations of 1.2 mg/mL. Eight and 16 scans from 190 to 260 nm and from 250 to 320 nm were averaged, respectively. Results were recorded in millidegrees and converted to mean residue ellipticity in degrees per square centimeter decimole.

To obtain spectra reflecting only the Trp contribution in various positions of TL, we subtracted the spectrum of W17Y, a mutant without Trp, from spectra of mutants with Trp17. The structural and binding characteristics of W17Y are similar to those of WT (*16*). The greatest difference in the amplitude of the near-CD spectra of W17Y versus the W17F is only 13% (data not shown). Therefore, the contribution of Tyr at position 17 in the calculated CD spectra is insignificant.

We estimated the distances between the midpoints of the CD2−CE2 bonds of the tryptophans in I98W using the value calculated for the most favorable orientation for maximum couplet strength which occurs when the indole rings are stacked, with the center to center vector perpendicular to each ring and one ring rotated by 45° with respect to the other (*23*).

To further check our approximations of distances between these tryptophan residues, the spectrum of exciton coupling was derived using the calculations of couplet strength between two tryptophans (*23*, *24*) in combination with the distances estimated from fluorescence (see below). Calculations of rotational strength R and interaction energy V_{ij} were performed and included only the B_b transition of the indole side chains. For pairwise interaction, this gives a simple exciton couplet centered at the wavelength of the transition in the isolated chromophore. The two exciton components have rotational strengths of the same magnitude. One calculates R from the equation

$$R = (\pi/2\lambda_i)\vec{R}_{ij}\cdot\vec{\mu}_{i0a} \times \vec{\mu}_{j0a}$$

where λ_i is the wavelength of the unperturbed transition, $\vec{R}_{ij}$ is the vector from the center of chromophore i to that of j, and $\vec{\mu}_{i0a}$ and $\vec{\mu}_{j0a}$ are the electric dipole transition moments for transition $0 \rightarrow a$ of groups i and j, respectively. The interaction energy was calculated by the point dipole approximation

$$V_{ij} = (R_{ij})^{-3}[\vec{\mu}_{i0a}\cdot\vec{\mu}_{j0a} - 3(\vec{\mu}_{i0a}\cdot\vec{R}_{ij})(\vec{\mu}_{j0a}\cdot\vec{R}_{ij})/R_{ij}{}^2]$$

Parameters for Trp residues were taken from refs *23* and *25*. The energy of the B_b transition was taken to be 5.5 eV ($\lambda_{max} = 225$ nm), and $|\vec{\mu}| = 5.7$ D. The center of the indole group was taken to be midpoint of the CD2−CE2 bond. To calculate CD spectra, a Gaussian band shape was assumed. The bandwidth parameter, half the width e^{-1} of the maximum, was calculated from each band from the empirical formula (*23*).

$$\Delta_i = k\lambda_i^{1.5}$$

The value of the parameter k was taken to be 0.0027, which gives a Δ_i of 9.1 nm for a λ_i of 225 nm (*23*, *25*). θ_{max} was calculated from the formulas (*24*)

$$R = 2.296 \times 10^{-39}\sqrt{\pi}\Delta\epsilon_{max}(\Delta_i/\lambda_i),\ \theta_{max} = 3298\Delta\epsilon_{max}$$

Experimentally, the couplet strength corresponds to the peak-to-trough difference in ellipticities of the couple, $S = \theta^{\alpha} - \theta^{\beta}$, where θ^{α} and θ^{β} are long- and short-wavelength lobes of the couplet, respectively. $\theta^{\alpha,\beta} = \theta_{max}\exp\{-[(\lambda - \lambda^{\alpha,\beta})/\Delta_i]^2\}$, and $\sigma^{\alpha,\beta} = \sigma_i \pm V_{ij}$, where σ is the wavenumber and σ_i is the wavenumber that corresponds to a λ_i of 225 nm.

Fluorescence Spectroscopy. Steady-state fluorescence measurements were taken on a Jobin Yvon-SPEX (Edison, NJ) Fluorolog tau-3 spectrofluorometer, where the bandwidths for excitation and emission were 2 nm. The excitation λ of 295 nm was used to ensure that light was absorbed almost entirely by tryptophanyl groups. Protein solutions with ~0.05 OD at 295 nm were analyzed. All spectra were obtained from samples in 10 mM sodium phosphate (pH 7.3). The temperature was maintained at 25 °C with a thermojacketed cell holder. The fluorescence spectra were corrected for light scattering from buffer and the instrument response using the appropriate correction curve.

The emission spectrum for I98W (Trp17, Trp98) in the absence of energy transfer was calculated as follows:

$$I_i^{Trp17,Trp98}(\lambda_i) = \alpha_{17}I_i^{Trp17}(\lambda_i) + \alpha_{98}I_i^{Trp98}(\lambda_i)$$

where α_{17} and α_{98} and $I_i^{Trp17}(\lambda_i)$ and $I_i^{Trp98}(\lambda_i)$ are normalized relative absorbances (at the excitation wavelength) and emission intensities, respectively, of the two separate corresponding tryptophan residues. A similar equation was used for calculation of emission spectra for F99W (Trp17, Trp99).

Time-resolved intensity decay data were obtained using a Jobin Yvon-SPEX Fluorolog tau-3 phase/modulation frequency domain fluorometer equipped with a 450 W xenon lamp as a light source. The excitation wavelength was set at 295 nm. Emission was observed through a Corning 7-57 filter. The light was modulated by a Pockels cell modulator. The available frequency range was 0.1−310 MHz. P-Terphenyl in ethanol was used as a reference standard (τ = 1.05 ns). Data analyses were performed with nonlinear least-squares programs from SPEX or from the Center for Fluorescence Spectroscopy (M. L. Johnson), University of Maryland at Baltimore, School of Medicine (Baltimore, MD). The goodness of fit was assessed by the χ^2 criterion (χ^2 ranged from 1.2 to 3.0).

No significant difference was detected with and without the "magic angle" condition in the fitted τ_i values. Therefore, the magic angle condition was not used for most intensity decay measurements.

The intensity decay data were analyzed in terms of the following multiexponential decay law:

$$I(t) = \sum_i \alpha_i \exp(-t/\tau_i)$$

where α_i and τ_i are the normalized preexponential factor and decay time, respectively. The fractional fluorescence intensity of each component is defined as $f_i = \alpha_i\tau_i/\sum\alpha_j\tau_j$.

The mean lifetime was calculated as $\bar{\tau} = \sum_i f_i\tau_i$. For calculation of the efficiency of RET, the amplitude-averaged lifetime $\langle\tau\rangle$ ($=\sum_i\alpha_i\tau_i$) was used.

RET between Trp Residues. RET between Trp residues was calculated according to the method of Eftink et al. (*26*). For example, the fluorescence quantum yield of mutant I98W (Trp17, Trp98) containing two Trp residues was compared with the sum of yields of WT (Trp17) and W17Y/I98W (Trp98) containing a single Trp residue. In the absence of RET between the tryptophan residues, the quantum yield, ϕ, is expected to be equal to $\alpha_{17}\phi_{17} + \alpha_{98}\phi_{98}$, where ϕ_{17} and ϕ_{98} are the quantum yields of Trp17 and Trp98, respectively, and α_{17} and α_{98} are the normalized relative absorbances of the two separate tryptophan residues at the excitation wavelength. From corrected absorbance spectra, we calculated α_{17} and α_{98} to be 0.61 and 0.39, respectively, at an excitation wavelength of 295 nm. The efficiency of energy transfer, E_T, from Trp98 to Trp17 was calculated by the following equation, assuming that the environments of Trp17 and Trp98 are the same when they are together in mutant I98W (*26*):

$$\phi = \alpha_{98}\phi_{98}(1 - E_T) + \alpha_{17}\phi_{17}(1 + E_T\alpha_{98}/\alpha_{17}).$$

An analogous formula was used for calculation of the efficiency of energy transfer from $\langle\tau\rangle$ values. The normalized relative absorbances of the tryptophan residues at positions 17 and 99 for mutant F99W containing both Trp residues were calculated to be 0.60 and 0.40, respectively, at an excitation wavelength of 295 nm.

According to Förster's theory (*27*), the efficiency of radiationless energy transfer, *E*, between a donor, D, and an acceptor, A, is given by

$$E = \frac{{R_0}^6}{{R_0}^6 + R^6}$$

where *R* is the distance between the donor and the acceptor. The distance R_0 (in angstroms) at which 50% energy transfer occurs is obtained from

$${R_0}^6 = 8.79 \times 10^{-5}[\kappa^2 n^{-4}\phi_D J(\lambda)]$$

The refractive index, *n*, of the medium is taken to be 1.5 (*28*). ϕ_D is the quantum yield of the donor in the absence of the acceptor.

The orientation factor, κ^2, describing the relative orientation of the transition dipoles of the donor and acceptor is calculated from

$$\kappa^2 = (\cos\theta_T - 3\cos\theta_D\cos\theta_A)^2$$

where θ_T is the angle between the emission dipole of the donor and the absorption dipole of the acceptor and θ_D and θ_A are the angles between these dipoles and the vector joining the midpoints of the CE2−CD2 bond of the donor and the acceptor, respectively. The direction of the transition moment of the L_a state is situated −38° from the longest axis in tryptophan (*29*). The structural model of TL (*12*) was assessed to compare it with experimental data. The side chain conformation of the conserved Trp17 was modeled as in β-lactoglobulin which is conserved for the lipocalin family. Six rotamers for Trp98 were analyzed. Optimization of the TL structure with tryptophan rotamers was performed by energy minimization as previously described except that 200 steps of steepest descent were followed by 200 steps of conjugate gradient descent (*12*). Four rotamers were excluded because of positive couplet strength and Trp B_b transition moments, and an $\vec{R}_{ij}$ value connecting the midpoint of the chromophore constitutes right-handed screwness. The relative orientation of Trp residues where the distance between Trp17 and Trp98 is 9.1 Å as measured from their geometric centers ($\kappa^2 = 0.77$; Figure 1) best characterizes both fluorescence energy transfer and Trp−Trp couplet strength.

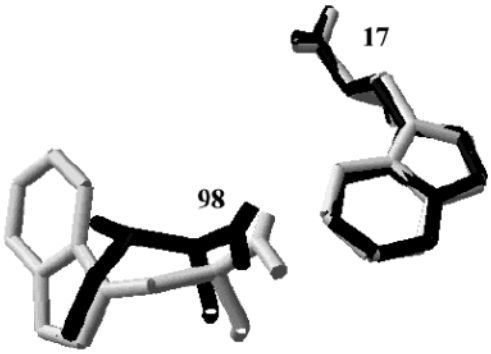

FIGURE 1: Orientation of positions 17 and 98 in TL (black) and I98W (gray) models. Modified from the homology model of TL (*12*). The distance between midpoints of the tryptophans is 9.1 Å.

The absorption spectra for Trp17 and Trp98 were obtained by spectral subtraction (WT − W17F and W17Y/I98W − W17Y, respectively).

To calculate the spectral overlap integral, $J(\lambda)$, it was necessary to construct the blue side of the Trp emission spectra. The spectrum of an elementary component on the wavelength (nanometers) scale can be described by a biparametric (maximum amplitude and position) log-normal function (*30*). The log-normal function (*30*) is fitted to Trp emission spectra, and the obtained parameter was used to construct the blue side of the spectra:

$$I(\lambda) = I_m \exp\left[-\frac{\ln 2}{\ln^2 p}\ln^2\left(\frac{a - 1/\lambda}{a - 1/\lambda_m}\right)\right]$$

where $I_m = I(\lambda_m)$ is the maximal fluorescence intensity, λ_m is the wavelength of the band maximum, $p = (1/\lambda_m - 1/\lambda_-)/(1/\lambda_+ - 1/\lambda_m)$ and is the band asymmetry parameter, $a = 1/\lambda_m + (1/\lambda_+ - 1/\lambda_-)p/(p^2 - 1)$ and is the function-limiting point, and $\lambda_+ = 10^7/(0.831 \times 10^7/\lambda_m + 7070)$ and $\lambda_- = 10^7/(1.177 \times 10^7/\lambda_m - 7780)$, where λ_+ and λ_- are the wavelength positions of half-maximal amplitudes. In some cases for better fitting, a second component was added.

Spectral overlap integral $J(\lambda)$ (in M^{-1} cm^{-1} nm^4) between the emission spectrum of the donor $F_D(\lambda)$ and the absorption spectrum of the acceptor $\epsilon_A(\lambda)$ is defined as

$$J(\lambda) = \frac{\int F_D(\lambda)\epsilon_A(\lambda)\lambda^4\,d\lambda}{\int F_D(\lambda)\,d\lambda}$$

Steady-State Fluorescence Anisotropy Measurements. Steady-state fluorescence anisotropy measurements were performed using a Jobin Yvon-SPEX automated L-format polarization accessory (Glan-Thompson polarizers). The bandwidths for excitation and emission were 2 and 6 nm, respectively. All anisotropy experiments were carried out at 22 °C.

The fluorescence anisotropy was calculated as follows:

$$r = (I_V - GI_H)/(I_V + 2GI_H)$$

where I_V and I_H are the fluorescent intensities of the vertically and horizontally polarized components, respectively, when excited with vertically polarized light. G is a correction factor and is equal to H_V/H_H, where H_V and H_H are the vertically and horizontally polarized components of fluorescence, respectively, when excited with horizontally polarized light. Values of G were measured for each set of λ_{ex} and λ_{em} (295 and 340 nm, 300 and 340 nm, and 305 and 345 nm). All measured fluorescence intensities were corrected for light scattering from buffer. The accuracy of the polarizer's alignment was checked by anisotropy values of scattered light using a dilute suspension of glycogen. The measured values ≥ 0.98. The anisotropy of NATA ≤ 0.005 in buffer at pH 7.3.

The fluorescence spectral center of mass (SCM; average emission wavelength) was calculated as

$$\mathrm{SCM} = \sum \lambda_i^{-2} I(\lambda_i) / \sum \lambda_i^{-3} I(\lambda_i)$$

where $I(\lambda_i)$ is the fluorescence intensity at wavelength λ_i that was sampled in 0.5 nm intervals.

RESULTS

Electron Paramagnetic Resonance-Monitored Ligand Binding. The results of ligand binding after substitution of tryptophan for native amino acids are shown in Figure 2. The composite spectra demonstrate the signals of free and bound C12SL monitored by high-field resonance peaks (Figure 2A). Free C12SL gives rise to a narrow peak, while the bound ligand yields a broad immobilized component. The spectra are quite similar for apo-WT and F99W. The dissociation constants (K_d) and stoichiometry are derived from the Scatchard plots of C12SL binding to each mutant (Figure 2B). All mutants show a level of binding of C12SL within the same order of magnitude as that of apo-WT (Figure 2B).

Circular Dichroism. The far-UV circular dichroism spectra of WT (Trp17), W17F (no Trp), W17Y (no Trp), W17Y/I98W (Trp98), and I98W (Trp17, Trp98) are shown in Figure 3A. The spectrum of WT is similar to that of W17Y and W17F except in the 220−235 nm region. In this region, there is increased optical activity indicating a positive contribution from Trp17 in WT. The rotational strength of aromatic residues interacting with the nearest neighbor peptide group can significantly contribute to the optical activity between 220 and 230 nm (*25*). The mutant W17Y/I98W with a single Trp98 shows less optical activity in the 210−225 nm region than WT (Trp17). This difference and the formation of new minima at 208 nm may be due to the distortion of secondary structure and/or an aromatic residue contribution. A dramatic difference is observed in the 220−245 nm region with I98W (mutant with tryptophans at 17 and 98). There is a marked increase in optical activity compared to mutants without tryptophan as well as those with a single tryptophan. The difference CD spectra (Figure 3A, inset) show a positive contribution to rotary strength at 219 nm and a negative contribution at 231 nm. The midpoint of these extremes is centered at 225 nm, indicating an exciton spectrum for the

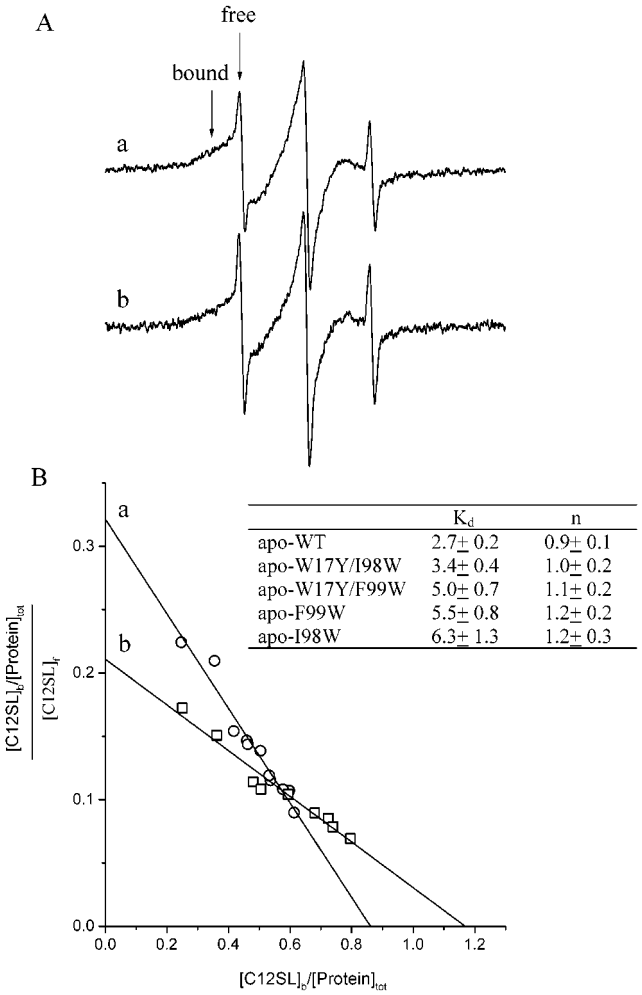

	K_d	n
apo-WT	2.7± 0.2	0.9± 0.1
apo-W17Y/I98W	3.4± 0.4	1.0± 0.2
apo-W17Y/F99W	5.0± 0.7	1.1± 0.2
apo-F99W	5.5± 0.8	1.2± 0.2
apo-I98W	6.3± 1.3	1.2± 0.3

FIGURE 2: (A) EPR spectra of C12SL (31 μM) with apo-WT (62 μM) (a) and C12SL (28 μM) with apo-F99W (54 μM) (b). (B) The dissociation constants and stoichiometry for each mutant are shown in the table. Scatchard plot of C12SL binding to apo-WT (a) and apo-F99W (b) where $[C12SL]_b$ is the concentration of bound ligand, $[C12SL]_f$ is the concentration of free ligand, and $[protein]_{tot}$ is the concentration of total protein. The experiments were performed in 10 mM phosphate buffer (pH 7.3).

B_b band of two tryptophan residues. According to Grishina (*23*), when two tryptophans are separated by 4.5 Å, the maximum strength is predicted to be as large as 2×10^6 deg cm^{-2} dmol^{-1}. For TL, with 158 residues, the molar ellipticity per residue becomes 12 658 deg cm^{-2} dmol^{-1}. Because couplet strength decreases as R^{-2}, the couplet strength of 2520 deg cm^{-2} dmol^{-1} (Figure 3A, inset) corresponds to a distance of 10 Å between tryptophans in the most favorable orientation. This implies that the distance between Trp17 and Trp98 is ≤10 Å. The calculated exciton spectrum for Trp17 and -98 in I98W (orientation in Figure 1 and distance of 9.3 Å as determined from fluorescent data; see below) is shown in the inset of Figure 3A. The calculated spectrum closely approximates the observed data, verifying the estimation of distances above.

Figure 3B shows the far-UV spectra of WT (Trp17), W17Y, W17F (no Trp), W17Y/F99W (Trp99), and F99W (Trp17, Trp99). The spectrum of W17Y/F99W is minimally altered from the spectra of W17Y and W17F. There is little contribution from Trp99 in the 220−250 nm region. In addition, the difference CD (Figure 3B, inset) shows no evidence to support an exciton effect. The lack of an exciton

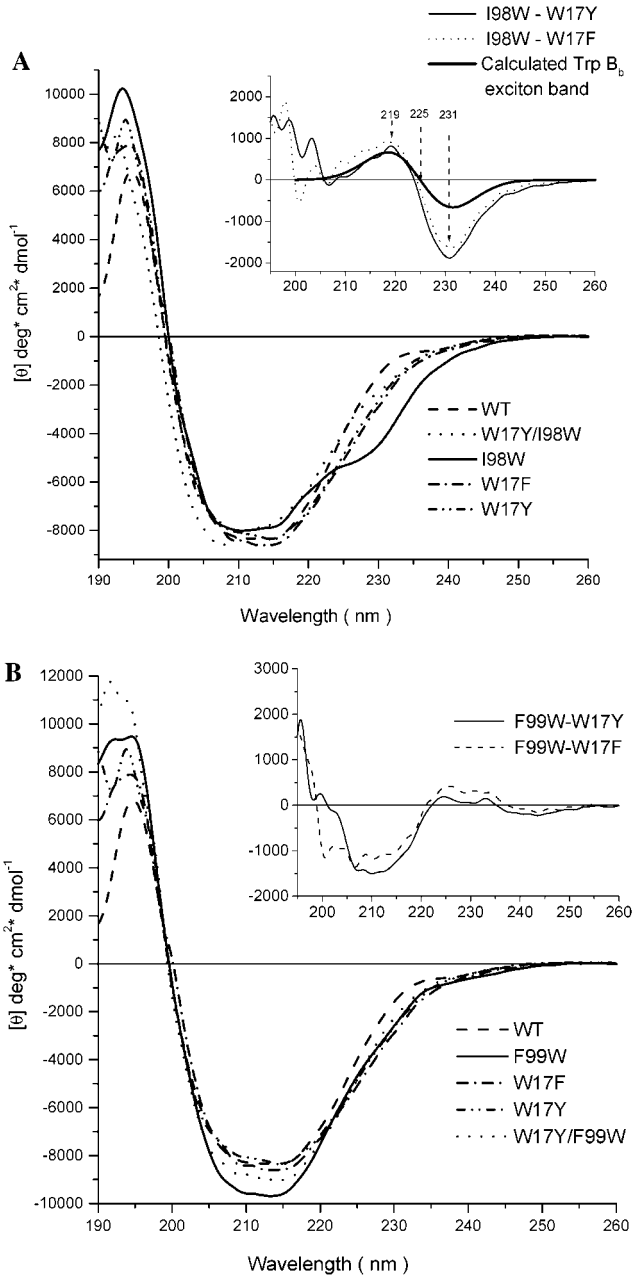

FIGURE 3: (A) Far-UV CD spectra of Trp mutants of TL for position 98. WT and tryptophanless mutants are shown for comparison. The inset shows difference CD spectra of the double tryptophan mutant I98W (Trp17, Trp98), the mutants without tryptophan, and the calculated Trp B_b exciton band for Trp17 and Trp98. (B) Far-UV CD spectra of Trp mutants of TL for position 99. WT and tryptophanless mutants are shown for comparison. The inset shows difference CD spectra of the double tryptophan mutant F99W (Trp17, Trp99) and the mutants without tryptophan.

effect does not exclude the proximity of chromophores, as the relative orientation may not permit excited-state interactions (*23*).

Steady-State Fluorescence Data. The fluorescence spectra of WT (Trp17), W17Y/I98W (Trp98), and I98W (Trp17, Trp98) are shown in Figure 4A. WT has a maximum emission at ~332 nm. W17Y/I98W is blue shifted in its emission maxima, and the fluorescent quantum yields are larger than that of the WT. Various fluorescence parameters of WT and mutant proteins are listed in Table 1. The fluorescence spectrum predicted for I98W (see Experimental Procedures) in the absence of energy transfer can be compared to the observed spectrum (Figure 4A).

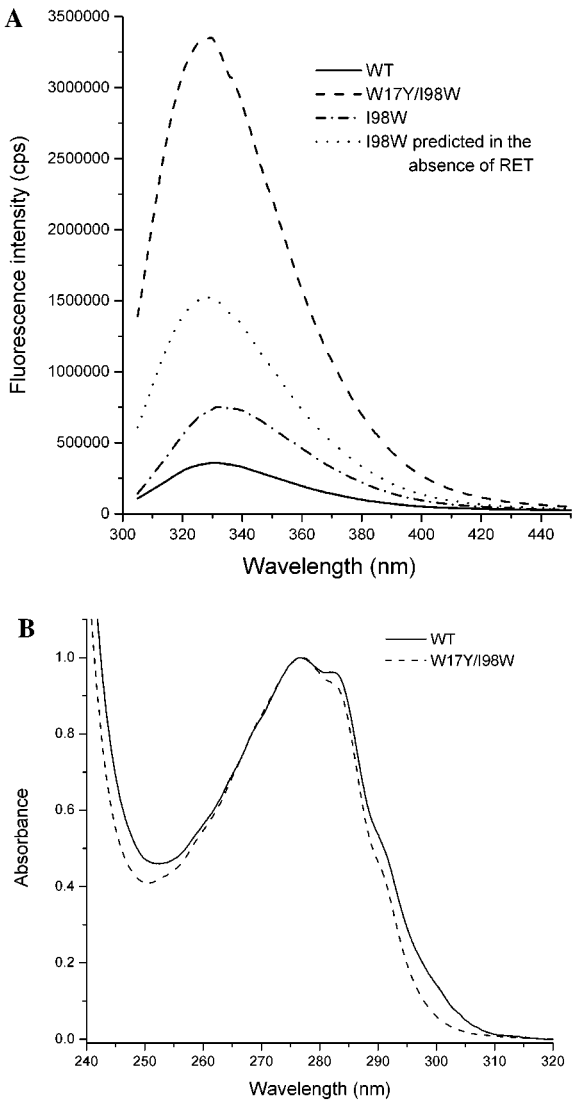

FIGURE 4: (A) Fluorescence spectra (corrected and normalized to an A_{295} of 0.05) of WT (Trp17), W17Y/I98W (Trp98), and I98W (Trp17, Trp98) and that predicted for I98W in the absence of energy transfer, assuming $\alpha_{17} = 0.61$ and $\alpha_{98} = 0.39$. (B) Absorbance spectra for WT (Trp17) and W17Y/I98W (Trp98).

Table 1: Fluorescence Parameters of WT and TL Mutants

	WT (Trp17)	W17Y/I98W (Trp98)	I98W (Trp17, Trp98)	W17Y/F99W (Trp99)	F99W (Trp17, Trp99)
λ_{max} (nm)	332	329	333	325	332
quantum yield	0.017	0.147	0.034	0.082	0.092
quantum yield[a]			0.068		0.043
τ_1 (ns)	0.24	1.15	0.59	0.76	0.92
α_1	0.97	0.26	0.95	0.59	0.58
f_1	0.72	0.09	0.80	0.25	0.32
τ_2 (ns)	3.6	4.05	2.85	3.22	2.76
α_2	0.03	0.74	0.05	0.41	0.42
f_2	0.28	0.91	0.20	0.75	0.68
τ_{mean}	1.18	3.79	1.04	2.61	2.17
$\langle\tau\rangle$	0.34	3.30	0.70	1.77	1.69
$\langle\tau\rangle^a$			1.49		0.91

[a] Predicted value for quantum yield or $\langle\tau\rangle$ in the absence of RET between Trp residues.

Figure 4B shows that the absorbance of Trp98 in mutant W17Y/I98W is blue shifted compared to that of Trp17 in

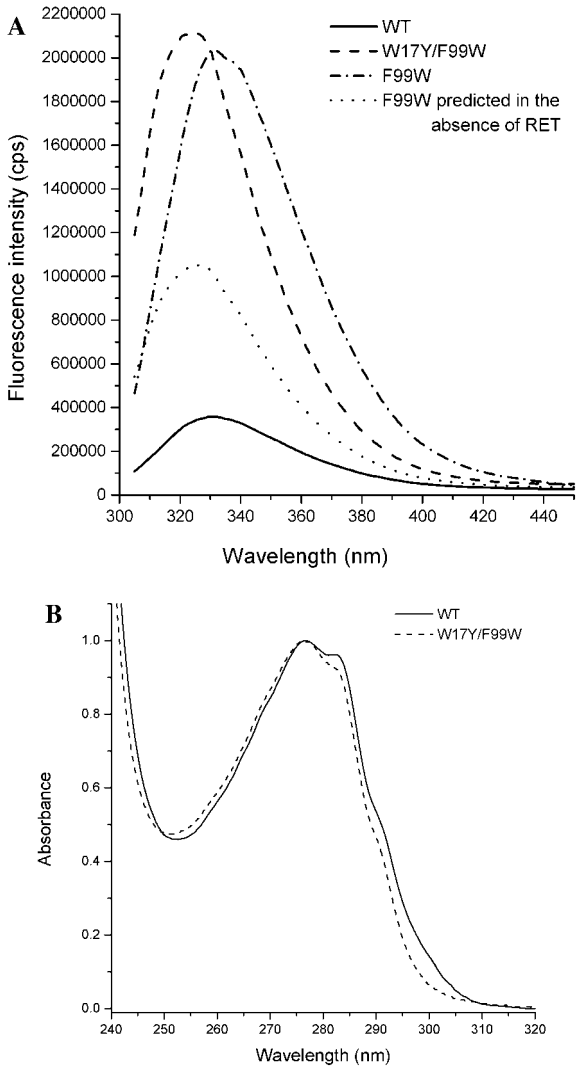

FIGURE 5: (A) Fluorescence spectra (corrected and normalized to an A_{295} of 0.05) of WT (Trp17), W17Y/F99W (Trp99), and F99W (Trp17, Trp99) and that predicted for F99W in the absence of energy transfer, assuming $\alpha_{17} = 0.60$ and $\alpha_{99} = 0.40$. (B) Absorbance spectra for WT (Trp17) and W17Y/F99W (Trp99).

the wild type. This feature indicates that Trp98 has a more apolar environment than Trp17.

The fluorescence spectra of F99W (Trp17, Trp99), WT (Trp17), and W17Y/F99W (Trp99) are shown in Figure 5A. The emission maximum of mutant W17Y/F99W (Trp99) is blue shifted, and the fluorescent quantum yield is greater than that of WT (Table 1). The fluorescent spectrum for F99W (Trp17, Trp99) exhibits a peak at 332 nm with a shoulder at 337.5 nm. The observed fluorescence spectrum of F99W shows a marked increase in quantum yield and is red shifted compared to that predicted in the absence of energy transfer. Figure 5B shows that the absorbance of Trp99 in W17Y/F99W is blue shifted compared to that of Trp17 in the wild type. As in case of Trp98, Trp99 also has a more apolar environment than Trp17.

Time-Resolved Fluorescence Data. Phase/modulation fluorescence lifetime data for WT and the two mutants are shown in Figure 6. In each case, the decay is nonexponential. The fitting parameters for biexponential decay are given in Table 1. The WT has contributions from both a 0.24 ns component and a 3.6 ns component. The decay of WT is dominated by a 0.24 ns component; the decay of W17Y/I98W is dominated

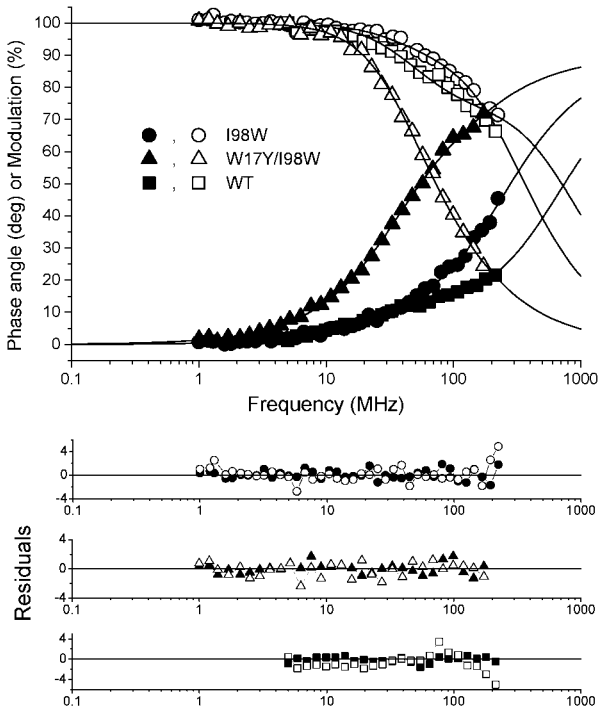

FIGURE 6: Phase angle (filled symbols) and modulation (empty symbols) fluorescence lifetime data for WT and position 98 mutants. Solid lines represent the best biexponential fit for the parameters given in Table 1.

by a 4.05 ns component, and the decay of I98W is dominated by a 0.59 ns component. In all three cases, there is a contribution from other components. In theory, in the absence of resonance energy transfer, the fluorescence decay of the mutant with two tryptophans reflects the sum of the combination of the decays of the two separate proteins each with a single tryptophan. The amplitude-averaged lifetime $\langle\tau\rangle$ for mutant I98W shows a value lower than that predicted in the absence of RET (Table 1).

The decay for W17Y/F99W (Trp99) is dominated by a 3.22 ns component and for F99W (Trp17, Trp99) a 2.76 ns component (Table 1). Both proteins show contributions from other components. In line with steady-state fluorescence, the amplitude-averaged lifetime for the mutant F99W shows a value greater than that predicted in the absence of RET.

The absorbance and emission spectra of Trp17 and Trp98 are shown in Figure 7. The overlap is more pronounced for direct transfer from Trp98 to Trp17 than the reverse. Values for the calculated distances R between the tryptophan residues in I98W, the orientation factors κ^2, and the overlap integrals J are shown in Table 2. κ^2 corresponds to the orientation shown in Figure 1. The lower overlap integral for Trp17 → Trp98 and the much lower quantum yield of Trp17 (Table 1) result in a lower R_0 value for energy transfer from Trp17 → Trp98 than from Trp98 → Trp17. For a distance of 9.3 Å between tryptophans, the efficiency of energy transfer from Trp17 → Trp98 would be 0.056 or 8% of the observed efficiency of energy transfer from Trp98 → Trp17. Therefore, energy transfer from Trp17 → Trp98 was excluded in the calculations of efficiency of energy transfer.

Steady-State Anisotropy Data. Steady-state anisotropy data for WT and mutants are shown in Figure 8. In every case, the anisotropy values rise with increasing excitation wave-

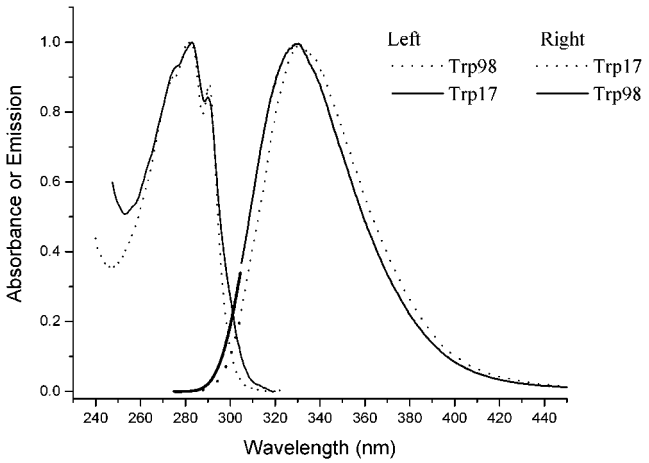

FIGURE 7: Spectra of absorbance (left) and emission (right) of Trp17 and Trp98. The blue sides of the emission spectra (bold solid and bold dotted lines) were constructed as a biparametric log-normal function (*30*). Solid lines show the overlap for RET from Trp98 to Trp17; dotted lines show the overlap for RET from Trp17 to Trp98.

Table 2: Calculated Distance R (Å), Orientation Factors κ^2, Overlap Integrals J ($\times 10^{11}$ M^{-1} cm^{-1} nm^4), and R_0 Values (Å) for Tryptophans in I98W

	Trp98 → Trp17	Trp17 → Trp98
R	9.3	
κ^2	0.77	0.77
J	6.66	1.72
R_0	10.4	5.8

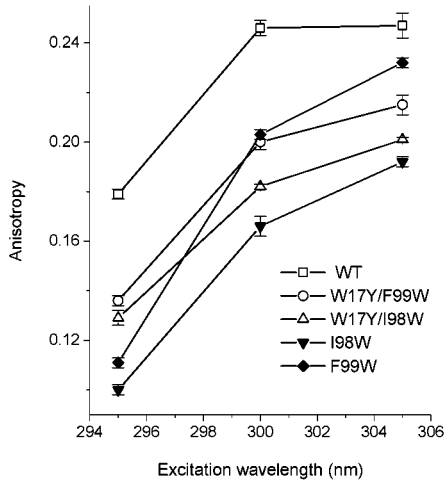

FIGURE 8: Anisotropy as a function of excitation wavelength of TL and its mutants.

length. WT (Trp17) shows the greatest value of anisotropy. W17Y/I98W (Trp98) has the lowest value of anisotropy among single-tryptophan mutants. The anisotropies of I98W (Trp17, Trp98) are lower than those of both WT and W17Y/I98W throughout the excitation wavelength range. There is a greater increase in anisotropy for I98W at 305 nm (92% increase over anisotropy at 295 nm) than for the single-tryptophan mutants (56% increase in anisotropy at 295 nm), although its value did not reach an intermediate value between that of WT and that of W17Y/I98W. The increase in anisotropy of F99W (Trp17, Trp99) is much greater than that of I98W with increasing excitation wavelength. The anisotropy of F99W at an excitation wavelength of 295 nm is lower than the anisotropies of both WT and W17Y/F99W, but at 305 nm, the anisotropy is intermediate between that of WT and that of W17Y/F99W.

DISCUSSION

Exciton Effect and the Proximity of Positions 17 and 98. Excited-state interactions between Trp17 and Trp98 give rise to a couplet CD band centered near 225 nm, an exciton effect. It is considered that the B_b band of Trp at 225 nm, the strongest transition in the indole group ($\epsilon_{max} \sim 35\,000$ M^{-1} cm^{-1}), is responsible for the main far-UV CD contribution (*23*). The magnitude and sign of B_b band CD strongly depend on both the backbone and side chain conformation. A special situation occurs when two Trp residues are in proximity. It is known that if two identical chromophores are sufficiently close, their excited states will interact to give rise to an exciton effect, which has a characteristic CD band called a couplet. Because the couplet strength decreases as R^{-2} (R is the distance between the geometric centers of the chromophores), the interaction is expected to be significant even at distances from 10 to 15 Å if the chromophores are favorably oriented (*23*). On the other hand, the strength of an exciton couplet depends on the square of the oscillator strength of the couplet chromophores and hence of ϵ_{max}. L_a (maximum at 275 nm) and B_b (maximum at 225 nm) bands of Trp have ϵ_{max} values of approximately 4500 and 35 000 M^{-1} cm^{-1}, respectively. Therefore, the Trp B_b band is ideally suited for detecting sterically close Trp−Trp pairs through exciton couplet formation. Such couplets have been observed in different proteins (*23*, *31*) and supported by theoretical calculations (*23*). The far-UV CD spectra of I98W, which has two Trp residues at positions 17 and 98, differ strikingly from those of other mutants with one or no Trp. Difference CD spectra show that the Trp17−Trp98 interaction gives a rise to negative couplet centered at 225 nm. The asymmetry observed for the exciton couplet may arise from the Tyr−Trp interaction (mutant W17Y/I98W) and/or from uncertainty in the determination of protein concentration. For example, a 7% increase in the intensity of the W17F CD spectrum results in an ideal symmetric couplet with a crossover at 225.3 nm. The exciton coupling is strong evidence that Trp17 and Trp98 are in proximity. The estimated maximal distance of 10 Å concurs with the distance obtained by fluorescence (9.3 Å). The calculated exciton spectra for 9.3 Å with the orientation chosen (Figure 1) corroborate the experimental data.

Resonance Energy Transfer. Resonance energy transfer from Trp98 to Trp17 is apparent in Figure 4A. The quantum yield of a Trp residue depends on its local environment and the proximity to a quenching group. Trp98 has a higher quantum yield than Trp17. Both the absorption and emission spectra of W17Y/I98W are blue shifted compared to that of WT. Therefore, Trp98 is exposed to a more apolar environment than Trp17 and is expected to be the donor in RET. The fluorescent quantum yield of the mutant I98W (Trp17, Trp98) is lower than that predicted from the sum of the quantum yield data for Trp17 and Trp98. The efficiency of energy transfer from Trp98 to Trp17 obtained from quantum yield data is 66 and 69% as obtained from $\langle\tau\rangle$ values. There is a significant increase in the short lifetime component (0.59 ns) in I98W compared to that of WT (0.24 ns). These data and the calculated R_0 values (Table 2) show that RET predominates from Trp98 → Trp17.

In proteins, for typical tryptophan−tryptophan RET with closely overlapping absorption and emission spectra, R_0 values are ~7−10 Å (*32*−*34*). κ^2, the orientation factor, depends on the relative orientation of the transition dipoles of the donor and acceptor (*32*−*35*). Estimation of the distance between Trp17 and -98 required knowledge of the correct side chain orientation. RET depends on the orientation of the L_a bands of tryptophan, but exciton coupling depends on the B_b bands. The directions of the L_a and B_b bands differ from each other so that one can choose the orientation which yields concordant results between the CD and fluorescence data. Six possible rotamers were examined. The derived exciton coupling spectra from four of these rotamers revealed positive couplets and were eliminated. Of the two remaining rotamers, one closely approximated our exciton coupling spectrum. In addition, the model constructed of this rotamer revealed an inter-tryptophan distance of 9.1 Å which closely matches our value for fluorescence data of 9.3 Å with the orientation shown (Figure 1).

The existence of RET between Trp17 and Trp99 is made complicated by the unusual fluorescence parameters of F99W (Table 1). The absorption and emission properties of Trp99 and Trp17 suggest that Trp17 is probably a RET acceptor (as in the case of I98W) in mutant F99W. F99W has a quantum yield that is greater than that predicted from the sum of the quantum yields of the individual tryptophans even in the absence of RET. These data are corroborated by lifetime measurements. The amplitude-averaged lifetime for F99W in the absence of energy transfer is predicted to be 0.91 ns, but the observed value is 1.69 ns. In addition, the emission spectrum of F99W shows a shoulder at 337.5 nm that was not observed in the presence of both Trp17 and Trp99. The most likely explanation is that the fluorescence quantum yield increased because the level of quenching by neighboring groups in the single-tryptophan mutant proteins was diminished in the mutant containing two tryptophans.

It is quite possible that the presence of both Trp17 and Trp99 produced conformational changes that resulted in a reduced level of quenching of one or both tryptophan residues by neighboring groups. It is most likely that Trp17 is responsible for an increased quantum yield in F99W because it accounts for most of the absorption (60%). In WT, Trp17 has a much lower quantum yield (0.017) than Trp99 (0.082) in W17Y/F99W. The far-UV CD data show little structural perturbation in the F99W mutant compared to proteins with single tryptophans at each site, suggesting that the overall structure is maintained. EPR data (Figure 2) show that F99W maintains ligand binding properties similar to those of other mutants and apo-WT. Analysis of the model generated from the secondary structure of TL confirms that the two residues are likely in proximity to permit such conformational interactions (*12*). Previous data suggest that Trp99 is more blue shifted than Trp98 and is oriented so that the side chain is pointed toward the interior of the cavity. Trp99 encounters an apolar environment and is constrained (*14*, *36*). The lifetime component of F99W, τ_1, was markedly increased, perhaps indicating a conformational shift of Trp17 occurred. However, the increased τ_1 of Trp17 could reflect both a conformational shift at Trp17 and energy transfer from Trp99 to Trp17. To establish the resonance energy transfer from Trp99 to Trp17, we performed anisotropy measurements.

Anisotropy Measurements. The steady-state anisotropy data show resonance energy transfer from both Trp98 and Trp99 to Trp17 (Figure 8). For any tryptophan excited at 305 nm, the maximum anisotropy is ~0.32 (*37*). Given the fluorescent lifetimes, the relatively high anisotropy values obtained for Trp17, Trp98, and Trp99 at the excitation wavelength of 305 nm suggest restricted mobility of their side chains. These data corroborate site-directed spin labeling work that showed the side chains of Trp98 and Trp99 are motionally constrained (*14*). Trp17, which has the highest anisotropy value, also has the lowest mean lifetime of fluorescence (Table 1). According to the Perrin equation (*32*), anisotropy is sensitive to both the fluorescent lifetime and the rotational correlation time of the fluorophore. The higher anisotropy value obtained for Trp17 compared to those of Trp98 and Trp99 does not necessarily imply that its side chain is more restricted. All anisotropy values increase with increasing excitation wavelength (Figure 8). This dependence is attributed to the two excited states of indole (L_a and L_b). The transition moments are perpendicular to each other, and the emission of Trp occurs mainly from the L_a state, which is red shifted compared to the L_b state. Therefore, the increase in the anisotropy toward the red edge of the absorption band is due to photoselection of the predominantly L_a transition, since there are small angular differences between the absorption and emission transition moments for L_a.

The anisotropies of I98W and F99W, each containing two Trp residues, have similar patterns with an increasing excitation wavelength, but there are important differences compared to the patterns of the single-Trp proteins. In the absence of energy transfer, anisotropy of a protein containing two Trp residues is given by $\bar{r} = f_1 r_1 + f_2 r_2$, where f_i and r_i represent the anisotropies and the fractional fluorescence intensities of the individual species, respectively. Therefore, in the absence of RET, the anisotropy values of mutants with two Trp residues are expected to have an intermediate value between those of the two separate proteins, each with a single Trp. At the excitation wavelength of 295 nm, anisotropies of I98W (Trp17, Trp98) and F99W (Trp17, Trp99) are substantially lower than those of both WT and W17Y/I98W and WT and W17Y/F99W, respectively (Figure 8). This indicates resonance energy transfer from Trp98 and Trp99 to Trp17. With the increase in excitation wavelength, a red edge excitation effect is produced, whereby the emission spectrum of the donor is red shifted to reduce the spectral overlap (reduced overlap integral) with absorption spectra of the acceptor (*32*). It is evident in Figure 8 that with the increase in the excitation wavelength to 305 nm, the anisotropy of F99W increases to an intermediate value between that of WT and W17Y/F99W. If the decreased value of anisotropy for F99W at the excitation value of 295 nm was due to a perturbation that changed the side chain mobility and/or fluorescence lifetime, then this change should be consistent throughout the range of excitation wavelengths that were tested. However, the relative increase in anisotropy with red edge excitation to an intermediate value between those of Trp17 and Trp99 clearly establishes the existence of resonance energy transfer at the excitation wavelength of 295 nm.

It is evident from Figure 8 that the response to the red excitation effect is greater in magnitude for F99W than for I98W (in both cases, resonance energy transfers to Trp17).

Table 3: Interatomic Distances between Residues That Constitute the Internal Hydrophobic Cluster in TL[a]

amino acid (atom)	amino acid (atom)	distance (Å)
V13 (CB)	W17 (CZ2)	3.85
M39 (CB)	W17 (CB)	4.83
L41 (CD2)	W17 (CD1)	3.98
F99 (CD1)	W17 (CZ2)	3.97
V116 (CG2)	W17 (CB)	3.47
L41 (CD2)	M39 (CB)	3.82
F99 (CB)	V116 (CG2)	4.30
F99 (CB)	I88 (CG1)	3.83
V116 (CG2)	L41 (CD2)	4.51
V116 (CG1)	L19 (CD2)	3.62
L19 (CD2)	M39 (SD)	4.10
L49 (CD2)	F99 (CZ)	3.81
L49 (CB)	Y77 (CD2)	3.79
A86 (CB)	Y77 (CB)	4.53

corresponding residues in β-lactoglobulin and TL that form the internal hydrophobic cluster

BLG	V15	W19	S21	V43	L46	L54	F82	V92	V94	L103	F105	L122
TL	V13	W17	L19	M39	L41	L49	Y77	A86	I88	F99	C101	V116

[a] Coordinates derived from the homology model for TL (*12*).

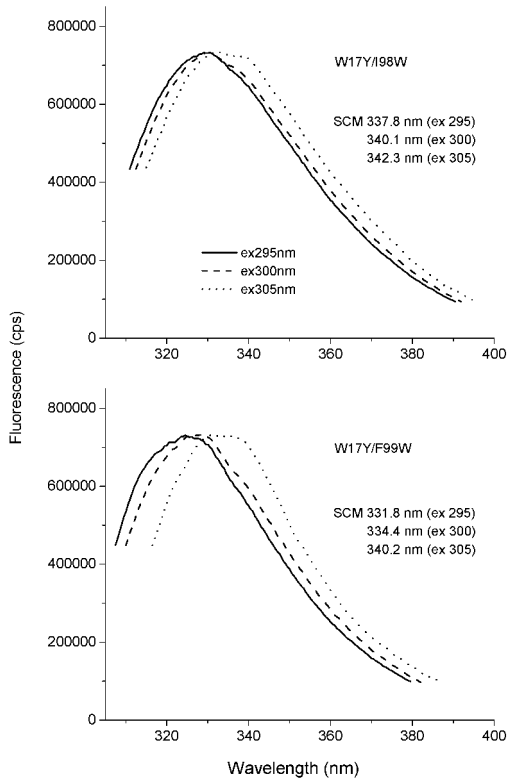

FIGURE 9: Red edge excitation effect for mutants with tryptophans at positions 98 and 99.

This difference can be related to the greater red edge excitation shifts of the emission spectra of W17Y/F99W (the red shift from 295 to 305 nm is 8.4 nm) compared to that for W17Y/I98W (the red shift from 295 to 305 nm is 4.5 nm) (Figure 9). The overlap integral is influenced mainly by the blue edge of the emission spectra of the donor. Inspection of Figure 9 reveals that the red shift differences are even greater at the blue edge of the spectra for W17Y/F99W and W17Y/I98W compared to that of SCM of the same spectra. Therefore, the spectral overlap is reduced more for F99W than for I98W, which accounts for the reduced level of resonance energy transfer between Trp residues in F99W at the excitation wavelength of 305 nm.

The anisotropy data also support the notion that the environment of tryptophan at position 99 in F99W is similar that of W17Y/F99W. Comparison of the spectra in Figure 9 shows an enhanced red excitation effect for W17Y/F99W compared to W17F/I98W and implies that position 99 is more sensitive to this effect than position 98 in the proteins with a single tryptophan. It is evident from Figure 8 that F99W displays a higher value of anisotropy at 305 nm than does I98W due to reduced spectral overlap (RET) at the longer excitation wavelengths and indicates that the emission of F99W is more red shifted than that of I98W. Hence, photoselection of the microstates of tryptophan at position 99 in W17Y/F99W that led to the increased sensitivity for the red excitation effect is retained in F99W. Furthermore, the anisotropy of F99W at 305 nm is intermediate between those of WT and W17Y/F99W (Figure 8), a result expected in the absence of RET. These findings are evidence against a major environmental/positional alteration of either Trp17 or Trp 99 in the F99W mutant despite the discrepancy between quantum yields of proteins containing one and two tryptophans.

Trp17 is close to the residues in positions 98 and 99 of tear lipocalin. These data provide direct experimental support for our homology model of TL (*12*) which places Trp17 only 3.97 Å from Phe99 (Table 3) and 5.53 Å [Trp17 (CZ3)−Ile98 (CB)] from Ile98. In the model, Phe99 is buried deep in the cavity, a position consistent with numerous previous observations (*13*, *14*, *36*). It is likely that Phe99 is part of a hydrophobic cluster in the cavity of TL.

The tryptophan in TL is a highly conserved residue in the lipocalin family, and it is logical that its impact on function would also be conserved. In β-lactoglobulin, NMR data identify 11 amino acid residues that point toward the interior and form a hydrophobic cluster centered around conserved Trp19 and including Leu103 (*10*). In the crystal structure of β-lactoglobulin, Trp19, Tyr102, and Leu103 are located in the closed end of the cavity. Despite the fact that Leu103 and Tyr102 face different sides of the cavity (internal and external, respectively), they are close to Trp19 [Trp19 (CH2)−Leu103 (CB) = 3.9 Å and Trp19 (CZ3)−Tyr102 (CB) = 4.9 Å (PDB entry 1B0O)].

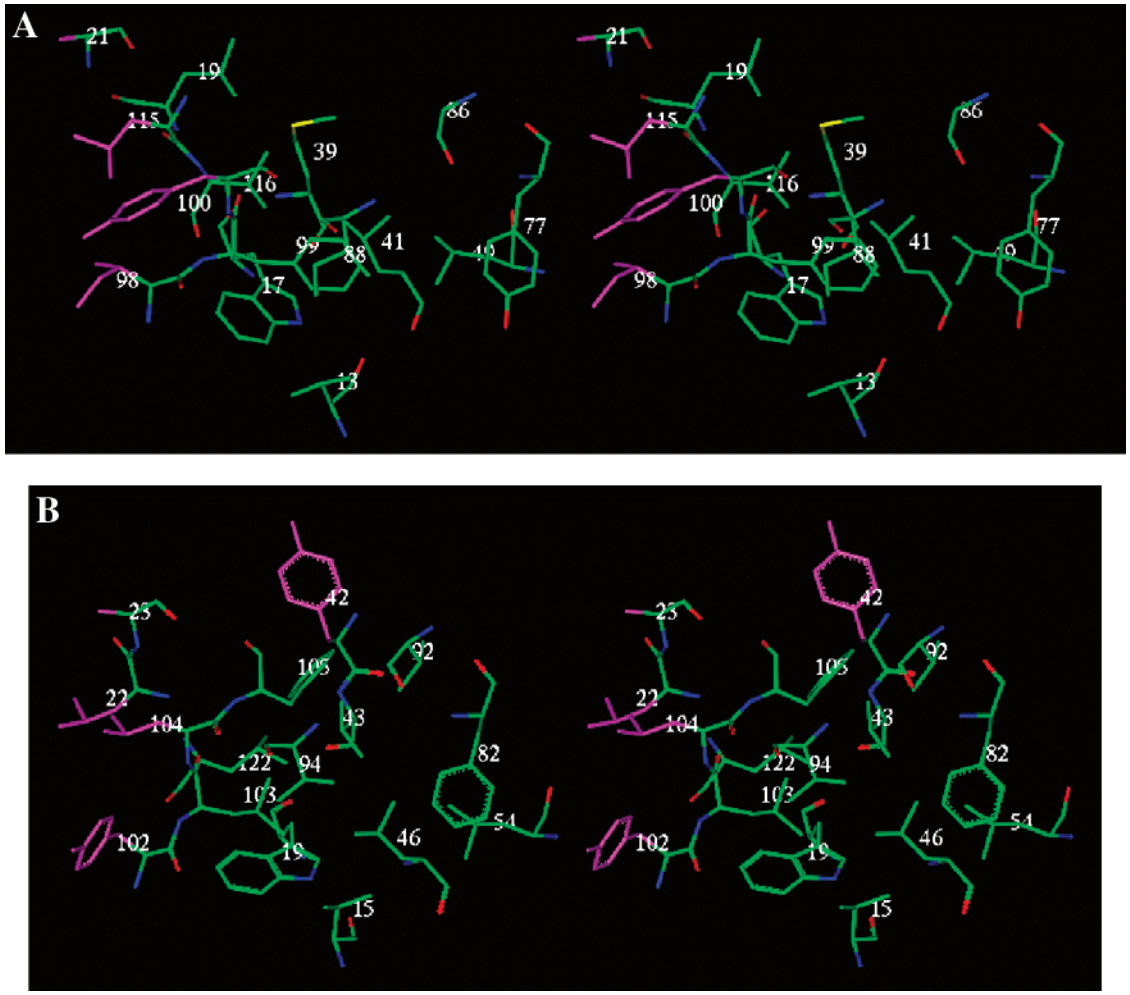

FIGURE 10: Residues that constitute the internal hydrophobic cluster (green, carbon; red, oxygen; blue, nitrogen; and yellow, sulfur) and external hydrophobic patch (magenta) of (A) tear lipocalin as derived from the homology model (*12*) and (B) β-lactoglobulin (PDB entry 1B0O).

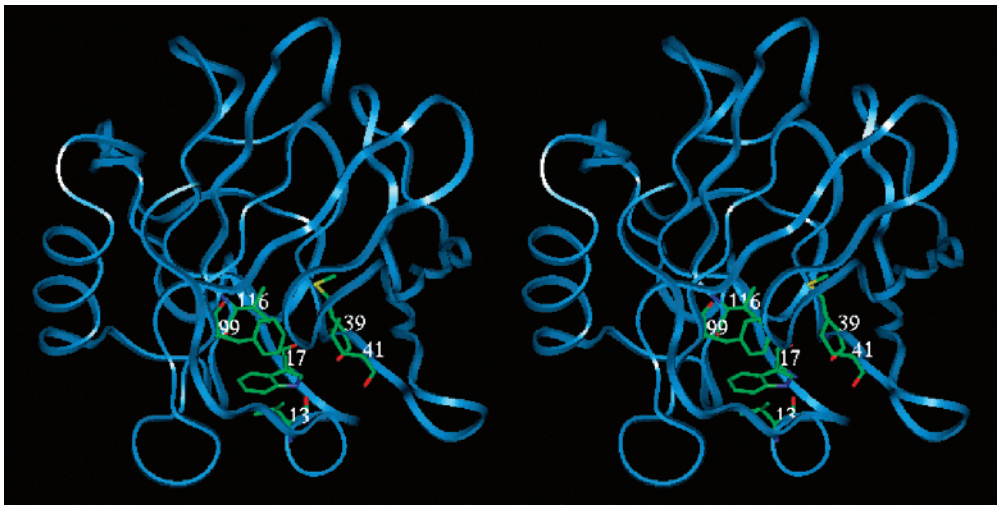

FIGURE 11: Stereodiagram of TL in a ribbon configuration with hydrophobic residues (red) proximal to Trp and side chains (green, carbon; red, oxygen; blue, nitrogen; and yellow, sulfur), with coordinates derived from the homology model (*12*).

The interior hydrophobic cluster and external hydrophobic patch for β-lactoglobulin can be compared with the homology model for TL (*12*) and the corresponding residues (Figure 10). The model of TL (Figure 10A) shows that the side chain of Ile98 (Tyr102 in β-lactoglobulin, Figure 10B) is oriented away from the cavity but close to Trp17. It is evident from Table 3 that Trp17 lies close to five hydrophobic residues; Trp17 forms the core of the internal hydrophobic cluster. In the model, Trp on strand A is proximate to hydrophobic residues on strands B, G, and H as well as the short α_{3-10} helix. The short interatomic distances for these residues are conducive to hydrophobic forces that would act to hold the strands and α_{3-10} helix together to form the closed tip of the calyx of TL (Figure 11). In addition to the analogous

Table 4: Interatomic Distances between Residues That Constitute the External Hydrophobic Patch in TL and Their Corresponding Residues in β-Lactoglobulin (PDB entry 1B0O)

amino acid (atom)	amino acid (atom)	distance (Å)
I98 (CG1)	Y100 (CE2)	3.59
L115 (CG)	Y100 (CE2)	3.99
L115 (CD1)	A21 (CB)	4.07

corresponding residues in β-lactoglobulin and TL that form the external hydrophobic patch						
BLG	L22	A23	Y42	Y102	L104	C121
TL	K20	A21	*a*	I98	Y100	L115

[a] No corresponding residue because strand B is truncated in TL.

residues for β-lactoglobulin, the interatomic distances from Leu19 to Met39 and Val116 in combination with the position in the 3D model of TL suggest that Leu19 is also a constituent of the hydrophobic cluster in TL. Ser21 is the corresponding residue in β-lactoglobulin and is not part of the hydrophobic cluster. Phe105 in the hydrophobic cluster of β-lactoglobulin corresponds to Cys101, which has a slightly polar side chain. In our model, Leu115 on strand H of TL bridges strands A and G to complete the external hydrophobic patch (Figure 10A and Table 4). In β-lactoglobulin, there is an apparent gap in the hydrophobic patch (Cys121 is the corresponding residue). Tyr42 in β-lactoglobulin has no corresponding residue in TL; the B strand is truncated. Despite these differences among the proteins, our data show that the general motifs of these two hydrophobic clusters are retained.

The proximity of key residues in TL and the close functional inter-relationships with Trp17 give credence to the concept that Trp17, Ile98, and Phe99 contribute to important conserved groups of hydrophobic residues. It is likely that the individual variations of these motifs will have important influences on the stability, conformation, and diversity of ligand binding of lipocalin family members.

ACKNOWLEDGMENT

We thank Dr. Joseph Horwitz for access to the CD instrument, Dr. Wayne Hubbell for C12SL and access to the Varian E109 instrument, and Christian Altenbach for his guidance in operating the Octane Silicon Graphics Workstation.

SUPPORTING INFORMATION AVAILABLE

Near-UV spectra of Trp mutants of TL for positions 98 and 99 and the difference spectra (protein − W17Y). This material is available free of charge via the Internet at http://pubs.acs.org.

REFERENCES

1. Glasgow, B. J., Abduragimov, A. R., Farahbakash, Z., Faull, K. F., and Hubbell, W. L. (1995) *Curr. Eye Res. 14*, 363−372.
2. Glasgow, B. J., Marshall, G., Gasymov, O. K., Abduragimov, A. R., Yusifov, T. N., and Knobler, C. M. (1999) *Invest. Ophthalmol. Visual Sci. 40*, 3100−3107.
3. Selsted, M. E., and Martinez, R. J. (1982) *Exp. Eye Res. 34*, 305−318.
4. van't Hof, W., Blankenvoorde, M. F. J., Veerman, E. C. I., and Amerongen, A. V. N. (1997) *J. Biol. Chem. 272*, 1837−1841.
5. Blaker, M., Kock, K., Ahlers, C., Buck, F., and Schmale, H. (1993) *Biochim. Biophys. Acta 1172*, 131−137.
6. Redl, B., Holzfeind, P., and Lottspeich, F. (1992) *J. Biol. Chem. 267*, 20282−20287.
7. Lechner, M., Wojnar, P., and Redl, B. (2001) *Biochem. J. 356*, 129−135.
8. Yusifov, T. N., Abduragimov, A. R., Gasymov, O. K., and Glasgow, B. J. (2000) *Biochem. J. 347*, 815−819.
9. Flower, D. R. (1996) *Biochem. J. 318*, 1−14.
10. Ragona, L., Pusterla, F., Zetta, L., Monaco, H. L., and Molinari, H. (1997) *Folding Des. 2*, 281−290.
11. Katakura, Y., Totsuka, M., Ametani, A., and Kaminogawa, S. (1994) *Biochim. Biophys. Acta 1207*, 58−67.
12. Gasymov, O. K., Abduragimov, A. R., Yusifov, T. N., and Glasgow, B. J. (2001) *Biochemistry 40*, 14754−14762.
13. Gasymov, O. K., Abduragimov, A. R., Yusifov, T. N., and Glasgow, B. J. (1997) *Biochem. Biophys. Res. Commun. 239*, 191−196.
14. Glasgow, B. J., Gasymov, O. K., Abduragimov, A. R., Yusifov, T. N., Altenbach, C., and Hubbell, W. L. (1999) *Biochemistry 38*, 13707−13716.
15. Gasymov, O. K., Abduragimov, A. R., Yusifov, T. N., and Glasgow, B. J. (1998) *Biochim. Biophys. Acta 1386*, 145−156.
16. Gasymov, O. K., Abduragimov, A. R., Yusifov, T. N., and Glasgow, B. J. (1999) *Biochim. Biophys. Acta 1433*, 307−320.
17. Glasgow, B. J., Heinzmann, C., Kojis, T., Sparkes, R. S., Mohandas, T., and Bateman, J. B. (1993) *Curr. Eye Res. 11*, 1019−1023.
18. Glasgow, B. J. (1995) *Graefe's Arch. Clin. Exp. Ophthalmol. 233*, 513−522.
19. Cormack, B. (1987) in *Current Protocols in Molecular Biology* (Ausubel, F. M., Ed.) Suppl. 15, pp 8.5.1−8.5.9, Greene Publishing Associates and Wiley-Interscience, New York.
20. Marston, F. A. O. (1987) A Practical Approach, in *DNA Cloning* (Glover, D. M., Ed.) Vol. III, p 62, IRL Press, Oxford, England.
21. Bozimowski, D., Artiss, J. D., and Zak, B. (1985) *J. Clin. Chem. Clin. Biochem. 23*, 683−689.
22. Hubbell, W. L., Froncisz, W., and Hyde, J. S. (1987) *Rev. Sci. Instrum. 58*, 1879−1886.
23. Grishina, I. B., and Woody, R. W. (1994) *Faraday Discuss. 99*, 245−262.
24. Harada, N., and Nakanishi, K. (1983) *Circular spectroscopy. Exciton coupling in organic stereochemistry*, pp 363−405, University Science Books, Mill Valley, CA.
25. Woody, R. W. (1994) *Eur. Biophys. J. 23*, 253−262.
26. Eftink, M. R., Ramsay, G. D., Burns, L., Maki, A. H., Mann, C. J., Matthews, C. R., and Ghiron, C. A. (1993) *Biochemistry 32*, 9189−9198.
27. Förster, T. (1948) *Ann. Phys. 2*, 55−75.
28. Desie, G., Boens, N., and De Schryver, F. C. (1986) *Biochemistry 25*, 8301−8308.
29. Yamamoto, Y., and Tanaka, J. (1972) *Bull. Chem. Soc. Jpn. 45*, 1362−1366.
30. Burstein, E. A., and Emelyanenko, V. I. (1996) *Photochem. Photobiol. 64*, 316−320.
31. Kuwajima, K., Garvey, E. P., Finn, B. E., Matthews, C. R., and Sugai, S. (1991) *Biochemistry 30*, 7693−7703.
32. Lakowicz, J. R. (1999) *Principles of Fluorescence Spectroscopy*, 2nd ed., Plenum Press, New York.
33. Steinberg, I. Z. (1971) *Annu. Rev. Biochem. 40*, 83−114.
34. Kuznetsova, I. M., Yakusheva, T. A., and Turoverov, K. K. (1999) *FEBS Lett. 452*, 205−210.
35. Selvin, P. R. (1995) *Methods Enzymol. 246*, 301−334.
36. Gasymov, O. K., Abduragimov, A. R., Yusifov, T. N., and Glasgow, B. J. (2000) *Protein Sci. 9*, 325−331.
37. Valeur, B., and Weber, G. (1977) *Photochem. Photobiol. 25*, 441−444.

BI0121003